Cyclotron-maser experiments in a periodic waveguide

E. Jerby* and G. Bekefi
Department of Physics and Research Laboratory of Electronics, Massachusetts Institute of Technology, Cambridge, Massachusetts 02139
(Received 21 June 1993)

A periodic-waveguide cyclotron maser is presented in this paper. In this device, a nonrelativistic electron beam undergoes a cyclotron interaction with traveling waves in an inductive periodic waveguide. Results of amplifier and oscillator experiments are presented. These experiments are conducted in the microwave regime (~ 10 GHz) with low-energy (< 10 keV), low-current (< 1 A) electron beams. Considerable amplification (> 10 dB) and rf power (~ 100 W) have been measured in the amplifier and oscillator experiments, respectively.

PACS number(s): 52.75.Ms, 42.52.+x, 52.35.Hr

I. INTRODUCTION

Cyclotron instabilities between orbiting electrons and electromagnetic radiation have been studied for many years [1]. Various cyclotron devices have been investigated, including cyclotron resonance masers (CRM) [2–4] gyrotrons [5,6], cyclotron autoresonance masers (CARM) [7,8], wiggler-free free-electron lasers [9], and others. In these devices, a relativistic electron beam subjected to a longitudinal magnetic field interacts with a fast electromagnetic wave propagating in a uniform waveguide. Here relativistic effects play a dominant role (azimuthal bunching, for instance, is intensified by relativistic electron mass variations caused by electromagnetic accelerating and decelerating forces).

Cyclotron interactions with *slow* electromagnetic waves have been proposed and studied in Refs. [10–15]. Various kinds of dielectric-loaded waveguides have been proposed in order to increase the cyclotron interaction bandwidth and to reduce the required electron-beam energy. For example, Ref. [13] reports on a dielectric-loaded slow-wave cyclotron experiment conducted at 6 GHz with 30–40-keV electron beam and ~ 2 kG axial magnetic field. Electronic gains of 30 dB were reported in both the slow- and the fast-wave operating regimes. The slow-wave cyclotron interaction is characterized by a wider frequency band and by a higher sensitivity to the electron-beam spread as compared to the fast-wave cyclotron interaction. Theoretical studies [12] show that the slow- and the fast-wave cyclotron interactions differ substantially from one another in their operating mechanism; the slow-wave cyclotron interaction is characterized predominantly by axial bunching whereas the fast-wave cyclotron interaction is dominated by azimuthal bunching.

In the present work we use an inductively loaded periodic waveguide, which consists of an array of metal posts in a rectangular waveguide as shown in Fig. 1(a). The use of a metallic periodic waveguide (sometimes called an *artificial dielectric* [16]) alleviates some of the difficulties of dielectric-loaded slow-wave cyclotron devices (in particular, the detrimental electrostatic charging of the dielectric by the electron beam). In our experiment a low-energy (< 10 keV) electron beam is injected on-axis into the periodic waveguide, where it then interacts with traveling waves. Measurements of amplification [17] and oscillation presented in this paper demonstrate the feasibility of a compact low-energy cyclotron-maser device.

The tuning relation of the cyclotron interaction with the fundamental spatial harmonic of the periodic waveguide is given in a simplified form by

$$\omega = \omega_c + v_e \beta_0(\omega) , \tag{1a}$$

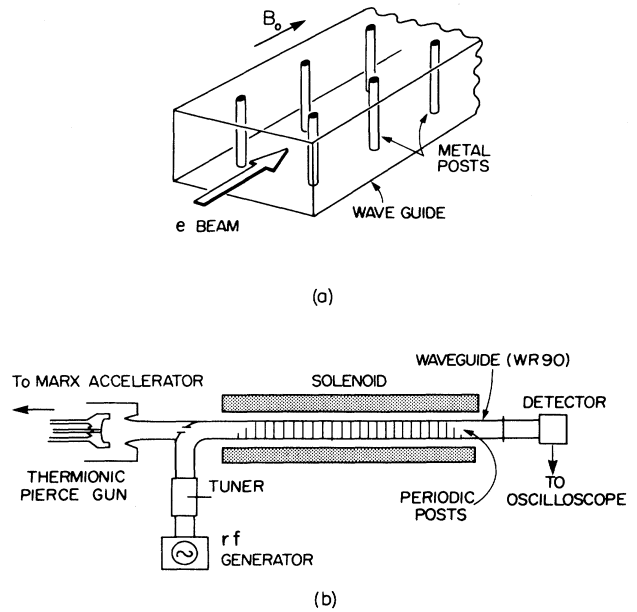

FIG. 1. A periodic-waveguide cyclotron scheme: (a) the metallic periodic structure; (b) the experimental setup for the amplifier experiment.

*Also at Faculty of Engineering, Tel Aviv University, Ramat Aviv 69978, Israel.

where ω is the electromagnetic wave angular frequency, v_e is the axial electron velocity, and $\beta_0(\omega)$ is the wave number; ω_c is the angular electron cyclotron frequency in the guide magnetic field β_0 and is given by $\omega_c = eB_0/\gamma m$, where e, m, and γ are the electron charge, mass, and relativistic energy factor, respectively.

The dispersion relation of the periodic waveguide [which determines the relation between β_0 and the frequency ω in Eq. (1a)] is given approximately by [16]

$$\cos(\beta_0 p) = \cos(k_{10} p) + \tfrac{1}{2}\bar{Y}\sin(k_{10} p)\ , \tag{1b}$$

where p is the period, $k_{10} = \sqrt{(\omega/c)^2 - (\pi/a)^2}$ is the wave number of the fundamental TE_{10} mode, and a is the waveguide width; $\bar{Y}$ denotes the normalized inductive susceptance of a single pair of posts in a uniform waveguide and is given approximately by

$$\bar{Y} = 2\phi_{10}^2(d)\phi_{10}^2(t)\left[k_{10}\sum_{n=3,5,\ldots}^{\infty}\frac{\phi_{n0}^2(d)\phi_{n0}^2(t)}{n^2\alpha_n}\right]^{-1}. \tag{1c}$$

Here $a_n = \sqrt{(n\pi/a)^2 - k^2}$ and $\phi_{n0}(x) = \sin(n\pi x/a)$ are the TE_{n0} mode decay rate and transverse profile, respectively, d is the distance between the post and the waveguide wall, and t is the radius of the metal post.

The tuning characteristics of the cyclotron interaction in the periodic waveguide are presented in Fig. 2 in the form of a dispersion diagram derived from Eqs. (1a)–(1c). It shows the intersection between the $\omega(\beta)$ dispersion relation of the periodic waveguide, Eq. (1b), and the electron cyclotron resonance line, $\omega = \omega_c + v_e\beta$ of Eq. (1a). The two beam lines shown in Fig. 2 correspond to the amplifier and oscillator experimental parameters presented in the following section. The dashed line illustrates the dispersion characteristics of the empty waveguide free of the metal posts. It will be noted that the resonance conditions [Eqs. (1a) and (1b)] are similar to those that govern CARM's [8] except that in this paper $\beta_0(\omega)$ is the wave number of the *periodic* system.

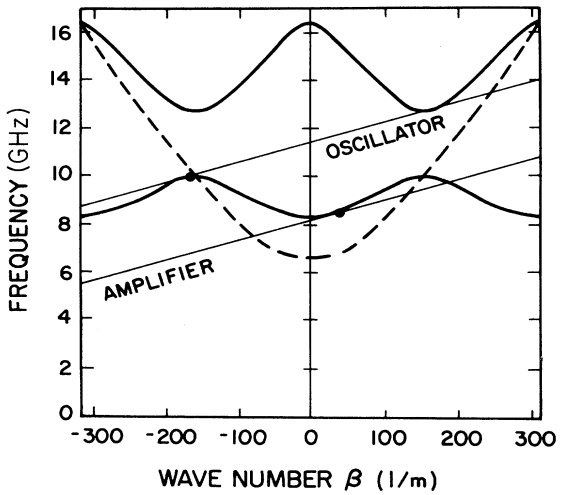

FIG. 2. A tuning diagram of the periodic-waveguide cyclotron interaction showing the dispersion curves of the periodic waveguide and two electron cyclotron resonance lines. The intersection points denote the operating points of the amplifier and oscillator experiments, respectively. The dashed line shows the empty waveguide dispersion curve.

II. EXPERIMENT

A schematic of the amplifier experimental setup is shown in Fig. 1(b). The accelerating potential is supplied by a Marx generator (Physics International Pulserad 615 MR). The pulsed electron beam is generated by a thermionically emitting, electrostatically focused, Pierce-type electron gun from a SLAC klystron (Model 343). An emittance selector is used to limit the beam current to ~1% of the total current of the gun. The initial electron-beam energy in this experiment is ~120 keV, and the voltage droop time constant is ~25 μs. The periodic-waveguide cyclotron interaction is observed, however, in a very-low-voltage range (1–10 keV).

An assembly of focusing coils transports the electron beam into the rectangular stainless-steel drift tube (1.02×2.29 cm^2). The beam is contained by a uniform axial magnetic field (3–4 kG) produced by a solenoid. No other means are used in this experiment to spin up the electron beam in order to acquire a transverse velocity component. The 2.7-m-long drift tube acts as a rectangular waveguide. A periodic array of posts is inserted into the waveguide as shown in Fig. 1, and forms a 1.7-m-long interaction region. The period of the periodic structure is 20 mm. The metal posts of the periodic waveguide are tapered at both ends in order to minimize reflections. The input microwave power from the driver (~1 mW) is injected as shown in Fig. 1(b) and tuned for a single frequency by a slide-screw tuner. The waveguide is terminated with a variable attenuator and a crystal detector (HP 423A) calibrated to 0.12 mW/mV (at 100 mV the detector response is slightly nonlinear). The output signals are recorded by a digital oscilloscope (HP 54510A).

The amplifier output as a function of time at a frequency of 8.2 GHz is shown in Fig. 3(a) together with the corresponding electron-beam energy trace. The axial magnetic field is 2.95 kG and the interaction occurs at a beam energy $V_{eb} \sim 9$ kV. This operating point is shown as a solid point on the amplifier line of Fig. 2. A slight increase in the axial magnetic field to 3.073 kG shown in Fig. 3(b) results in a smaller power output, and appears at a lower electron-beam voltage (~3 kV) in agreement with expectations [see Eq. 1(a)]. A slight decrease of B_0 results in a smaller gain as well, but at higher electron-beam energy.

Figure 4(a) shows the dependence in the amplifier experiment of peak output power on the axial magnetic field as measured at an input driver frequency of 8.2 GHz. It exhibits a resonance around 2.98 kG, which corresponds to a cyclotron frequency of 8.18 GHz. The corresponding dependence of the resonant electron-beam energy on the axial magnetic field is illustrated in Fig. 4(b). The spatial growth of the rf output as a function of the interaction length is given in Fig. 5. The cyclotron interaction in a uniform waveguide (with the periodic structure removed) was also measured under the same

conditions as above. Unlike the periodic-waveguide cyclotron results, the typical response of the uniform waveguide cyclotron was now characterized by a strong absorption of the wave.

Periodic-waveguide cyclotron characteristics in an oscillator rather than an amplifier configuration (with zero input signal from the driver) were studied in an independent experiment [18] at Tel Aviv University. A 0.5-m section of the periodic waveguide shown in Fig. 1 was used. The uniform axial magnetic field was produced by a solenoid; in addition, a short focusing "kicker" coil was wound on the waveguide at the entrance to the interaction region. Its field is superimposed locally on the solenoidal field near the electron gun and its purpose is to impart transverse velocity to the beam electrons. Considerable rf output is observed when this focusing coil is activated to ~5 (kA turns). The 0.25-A electron beam was

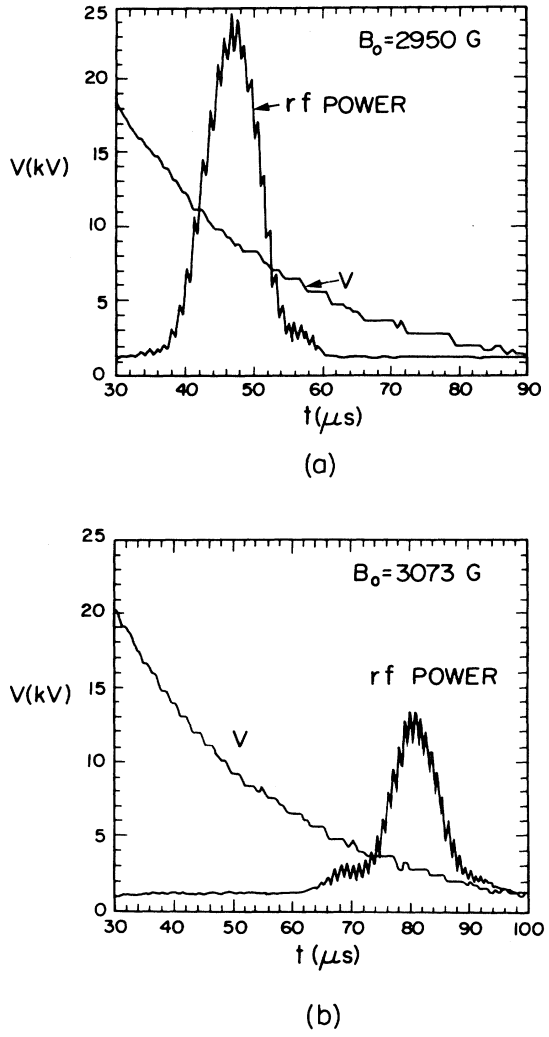

FIG. 3. rf output vs time of the periodic-waveguide cyclotron amplifier operating at 8.2 GHz, and the corresponding electron-beam voltage. (a) In an optimal magnetic field, $B_0 = 2950$ G. (b) In a slightly higher field, $B_0 = 3073$ G.

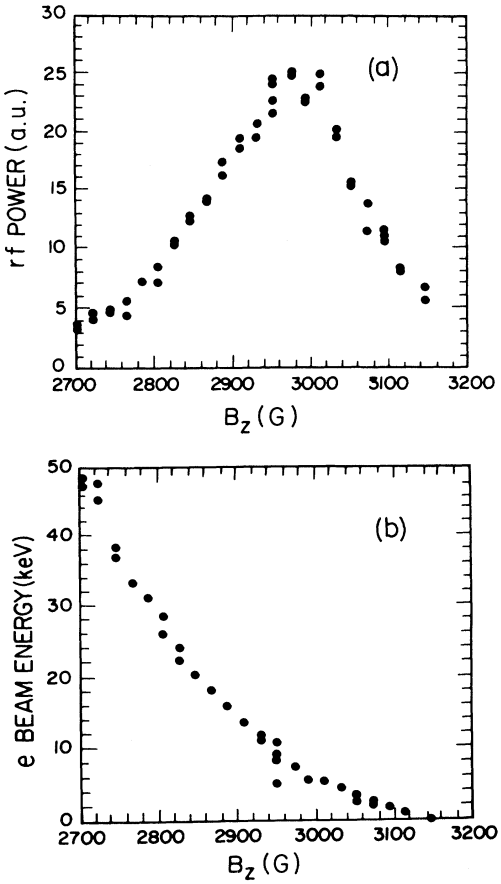

FIG. 4. (a) Maximum rf output of the amplifier, and (b) the corresponding electron-beam energy vs the axial magnetic-field strength.

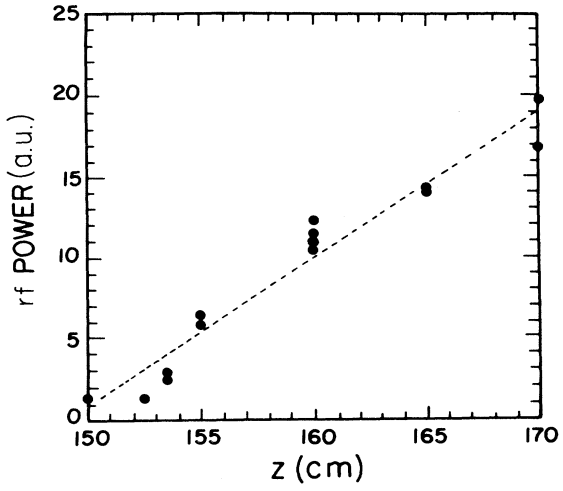

FIG. 5. Amplifier output vs the interaction length in the axial guide magnetic field.

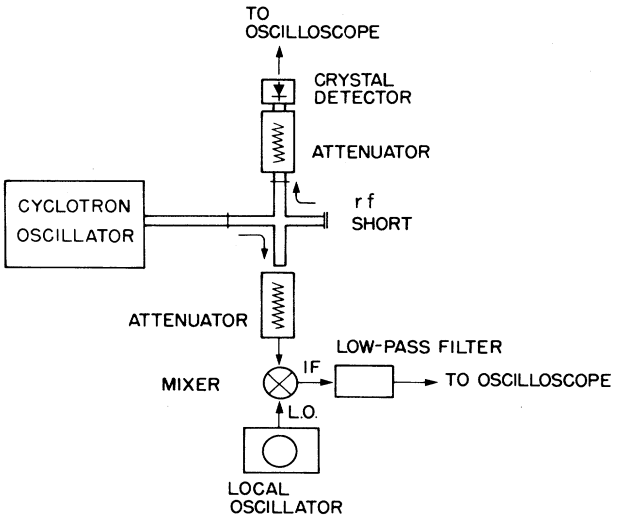

FIG. 6. Diagnostic setup of the periodic-waveguide cyclotron oscillator experiment.

generated by a thermionic cathode gun.

The rf power produced is detected by means of the apparatus shown in Fig. 6. The output signal is sampled by a 20-dB cross coupler and attenuated by a 30 dB attenuator in each arm. One arm measures the total rf power and the other arm is used to analyze the frequency characteristics of the oscillator. In this arm, the output signal is mixed with a 9.45-GHz fixed-frequency local oscillator. The mixer output is filtered by the internal 20-MHz low-pass filter of a Tektronix TDS 540 digital oscilloscope.

The mixed oscillator output is shown in Fig. 7(b) together with the electron-beam energy trace [Fig. 7(a)]. Two bursts of radiation are observed at approximately the same level of electron energy in the leading and the trailing edges of the electron voltage pulse. These bursts represent the sweep of the oscillator frequency (i.e., chirping) in the range 9.45 GHz±20 MHz due to electron energy variation. An expanded view of these two pulses in Figs. 7(c) and 7(d) shows clearly the variation of the oscillator frequency as a function of time. This frequency

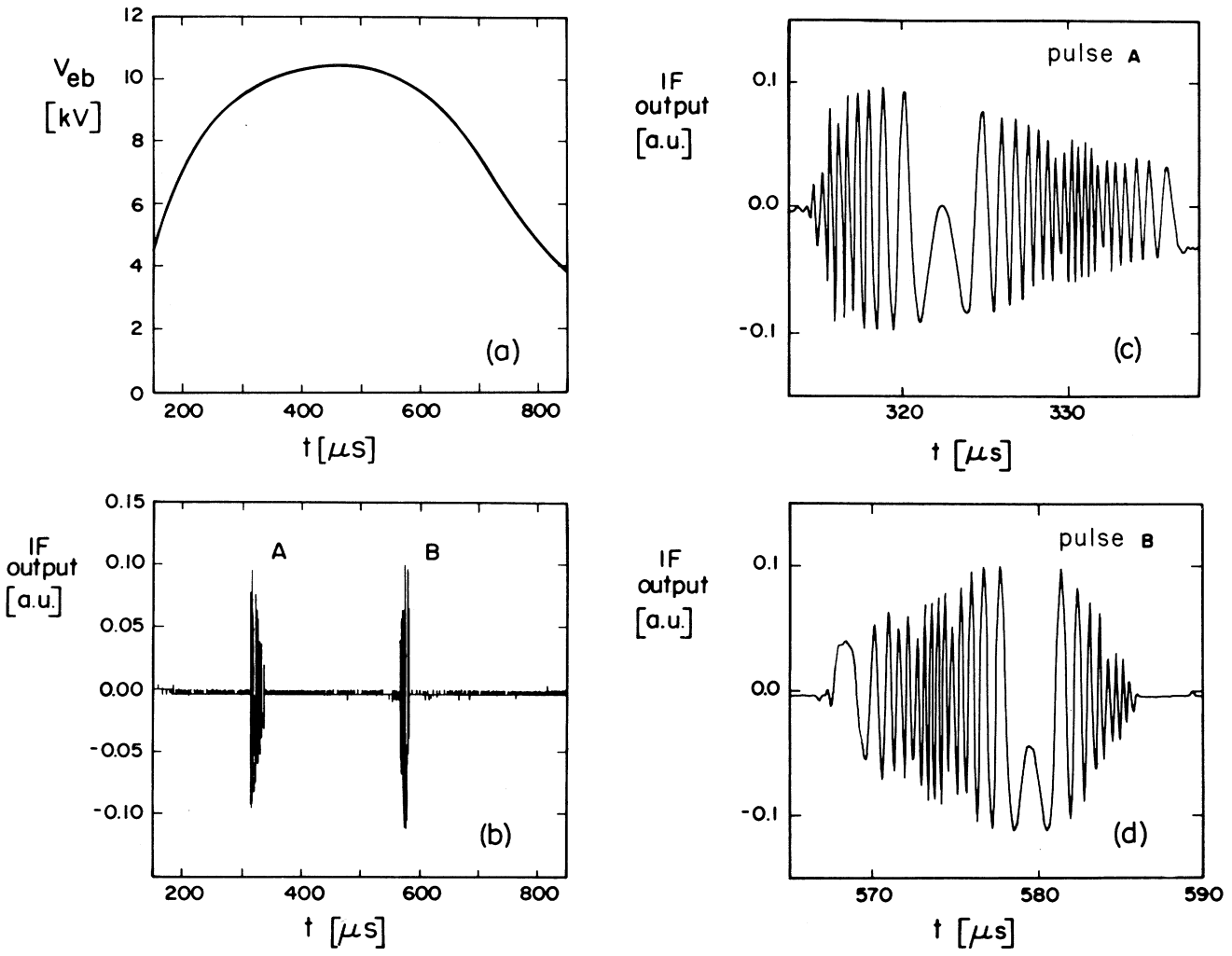

FIG. 7. (a) Beam energy and (b) mixer output vs time measured by the setup shown in Fig. 6 with $B_0=4.16$ kG and $f_{LO}=9.45$ GHz; (c) and (d) are expanded views of the output pulses A and B of Fig. (b).

chirp is a consequence of the electron energy sweep in the rise and fall times of the electron Gaussian pulse. The slow time dependence of the electron velocity $v_e(t)$ results in a corresponding sweep of the cyclotron resonance frequency $\omega(t)$ in accordance with the transcendental tuning equation $\omega(t)=\omega_c+V_e(t)\beta_0(\omega(t))$.

The rf power in the oscillator cavity measured by a crystal detector through a 20-dB coupler and a 30-dB attenuator is on the order of 100 W. The axial magnetic field is 4.16 kG, which corresponds to a cyclotron frequency of 11.4 GHz. The operating point of the cyclotron oscillator based on Eq. (1a) is marked as the second solid point shown in Fig. 2. We see that the periodic-waveguide cyclotron oscillator interacts with a *backward* spatial harmonic of the periodic structure, unlike the case of the amplifier.

III. DISCUSSION

The results of the periodic-waveguide cyclotron amplifier and oscillator experiments presented in this paper show strong interaction between a low-energy electron beam in an axial magnetic field and a traveling wave in a periodic waveguide. The coupling occurs near the cyclotron frequency. In the oscillator experiments a kicker magnet was used to impart transverse velocity to the electrons before entry into the interaction region. This confirms the usual expectations in cyclotronlike devices. In the amplifier experiment no such kicker was needed, presumably because the finite emittance from the gun provided sufficient transverse velocity in this series of experiments. However, a linear theoretical model of the periodic-waveguide cyclotron interaction [17] indicates that amplification (and oscillations) may also occur even without initial transverse electron velocity due to the inductive impedance of the periodic structure. This point will require more study.

Further theoretical and experimental studies are being conducted in order to evaluate the effects of the waveguide characteristics (impedance, dispersion, and losses) and the effect of the electron initial transverse velocity on the periodic-waveguide cyclotron interaction. These studies include other periodic waveguide structures in wider frequency ranges. The present amplifier and oscillator experiments demonstrate, however, the feasibility of a compact cyclotron-maser device operating with a low-energy electron beam in a periodic waveguide.

ACKNOWLEDGMENTS

This research was supported by the Air Force Office of Scientific Research, the Office of Naval Research, the Department of Energy, and the Israeli Ministry of Energy.

[1] R. Q. Twiss, Aust. J. Phys. **11**, 564 (1958).
[2] J. L. Hirshfield and J. M. Wachtel, Phys. Rev. Lett. **12**, 533 (1964).
[3] J. L. Hirshfield and V. L. Granatstein, IEEE Trans. Microwave Theory Tech. **25**, 522 (1977).
[4] P. Sprangle and A. T. Drobot, IEEE Trans. Microwave Theory Tech. **25**, 528 (1977).
[5] V. A. Flyagin, A. V. Gaponov, M. I. Petelin, and V. K. Yulpatov, IEEE Trans. Microwave Theory Tech. **25**, 514 (1977).
[6] J. M. Baird, in *High Power Microwaves,* edited by V. L. Granatstein and I. Alexeff (Artech House, Norwood, MA, 1987).
[7] V. L. Bratman, N. S. Ginzburg, G. S. Nusinovich, M. I. Petelin, and P. S. Strelkov, Int. J. Electron. **51**, 541 (1981).
[8] A. C. DiRienzo, G. Bekefi, C. Chen, and J. S. Wurtele, Phys. Fluids B **3**, 1755 (1991).
[9] A. Fruchtman and L. Friedland, IEEE J. Quantum Electron. **QE-19**, 327 (1983).
[10] K. R. Chu, P. Sprangle, and V. L. Granatstein, Bull. Am. Phys. Soc. **23**, 748 (1978).
[11] J. M. Baird, S. Y. Park, K. R. Chu, H. Keren, and J. L. Hirshfield, Bull. Am. Phys. Soc. **25**, 911 (1980).
[12] K. R. Chu, A. K. Ganguly, V. L. Granatstein, J. L. Hirshfield, S. Y. Park, and J. M. Baird, Int. J. Electron **51**, 493 (1981), and references therein.
[13] H. Guo, L. Chen, H. Keren, and J. L. Hirshfield, Phys. Rev. Lett. **49**, 730 (1982).
[14] A. K. Ganguly and S. Ahn, Phys. Rev. A **42**, 3544 (1990).
[15] K. C. Leou, D. B. McDermott, and N. C. Luhmann, Jr., IEEE Trans. Plasma Sci. PS-20, 188 (1992), and references therein.
[16] R. E. Collin, *Field Theory of Guided Waves* (McGraw-Hill, New York, 1960).
[17] E. Jerby and G. Bekefi in *Intense Microwave Pulses,* edited by H. E. Brandt, SPIE Proc. Vol. 1872 (SPIE, Bellingham, WA, 1993), p. 276.
[18] E. Agmon, H. Golombek, and E. Jerby, Nuclear Instrum. Methods A **331**, 156 (1993).